


Magnolia Officinalis Alcohol Extract Alleviates the Intestinal Injury Induced by Polygala Tenuifolia Through Regulating the PI3K/AKT/NF- κ B Signaling Pathway and Intestinal Flora

Si Liu, Dan Yang, Wen Li, Qiuping Chen, Danni Lu, Liang Xiong, Junjie Wu, Hui Ao, Lihua Huang 

State Key Laboratory of Southwestern Chinese Medicine Resources, School of Pharmacy, Chengdu University of Traditional Chinese Medicine, Chengdu, 611137, People's Republic of China

Correspondence: Lihua Huang; Hui Ao, College of Pharmacy, Chengdu University of Traditional Chinese Medicine, Chengdu, 611137, People's Republic of China, Email huanglihua@cudtcm.edu.cn; aohui2005@126.com

Purpose: *Polygala tenuifolia* Willd. (PT), a traditional Chinese medicinal plant extensively employed in managing Alzheimer's disease, exhibits notable gastrointestinal side effects as highlighted by prior investigations. In contrast, *Magnolia officinalis* Rehd. et Wils (MO), a traditional remedy for gastrointestinal ailments, shows promising potential for ameliorating this adverse effect of PT. The objective of this study is to examine the underlying mechanism of MO in alleviating the side effects of PT.

Methods: Hematoxylin-eosin (H&E) staining was used to observe the structural damage of zebrafish intestine, and enzyme-linked immunosorbent assay (ELISA) was used to detect the levels of inflammatory factors and oxidative stress. The integrity of the intestinal tight junctions was examined using transmission electron microscope (TEM). Moreover, the expression of intestinal barrier genes and PI3K/AKT/NF- κ B signaling pathway-related genes was determined through quantitative real-time PCR. The changes in intestinal microbial composition were analyzed using 16S rRNA and metagenomic techniques.

Results: MO effectively ameliorated intestinal pathological damage and barrier gene expression, and significantly alleviated intestinal injury by reducing the expression of inflammatory cytokines IL-1 β , IL-6, TNF- α , and inhibiting the activation of PI3K/AKT/NF- κ B pathway. Furthermore, MO could significantly increase the relative abundance of beneficial microorganisms (*Lactobacillus*, *Blautia* and *Saccharomyces cerevisiae*), and reduce the relative abundance of pathogenic bacteria (*Plesiomonas* and *Aeromonas*).

Conclusion: MO alleviated PT-induced intestinal injury, and its mechanism may be related to the inhibition of PI3K/AKT/NF- κ B pathway activation and regulation of intestinal flora.

Keywords: polygala tenuifolia, PI3K/AKT/NF- κ B, gut microbiota, inflammation, intestinal injury

Introduction

As a traditional Chinese medicine (TCM), *Polygala Tenuifolia* (PT, Yuan zhi in Chinese) is the dried root of *Polygala Tenuifolia* Willd. It has been widely utilized in the treatment of Alzheimer's disease, depression, anxiety, and insomnia.^{1,2} However, previous research has highlighted the severe gastrointestinal toxicity associated with PT, leading to gastrointestinal motility disorders, mucosal damage, and even death in mice.³⁻⁵ Additionally, saponins have been identified as the primary toxic components of PT, significantly hampering its application and development.⁶⁻⁸ *Magnolia Officinalis Cortex* (*Magnolia Officinalis* Rehd. et Wils, MO, Hou po in Chinese) has been extensively used in Asia for approximately 2000 years, primarily for the treatment of gastrointestinal diseases.⁹ Previous studies have explored the use of *Aurantii Fructus Immaturus*, *Acori Tatarinowii Rhizoma*, MO, and *Glycyrrhizae Radix et Rhizomawere* in addressing the gastrointestinal side effects of PT.^{2,10,11} Among these, MO has shown the most promising effect, although its mechanism of action remains unclear.

Increasing evidence suggests a significant correlation between the disruption of gut microbial homeostasis and gastrointestinal disorders.^{12–14} Intestinal microbial regulation may become a potential new protocol for preventing intestinal injury.¹⁵ MO exhibits a wide range of antibacterial activity, enabling it to resist the invasion of pathogenic microorganisms. Supplementation with magnolol can significantly increase the relative abundance of beneficial bacteria in weaned piglets.¹⁶ Magnolol can alleviate *S.pullorum*-induced intestinal villus structure damage by regulating intestinal flora.¹⁷ The efficacy of MO in regulating the composition of intestinal flora is acknowledged as a potent therapeutic approach for addressing intestinal damage.^{18,19}

Intestinal injury encompasses various aspects, including damage to the intestinal mucosal barrier and disruption of intestinal immune responses. This is primarily characterized by tight junction damage, disorders in the secretion of inflammatory factors, oxidative stress, and disruptions in intestinal flora.^{20,21} A substantial body of evidence suggests the involvement of the phosphoinositide 3-kinase/protein kinase B (PI3K/AKT) and nuclear factor kappa B (NF- κ B) pathways in the pathogenesis of gastrointestinal diseases.^{22–24} Additionally, network pharmacology predictions underscore the significance of the PI3K/AKT signaling pathway in gastrointestinal diseases.^{25,26} The PI3K/AKT pathway plays a crucial role in repairing intestinal mucosal damage by regulating the synthesis of intestinal tight junction proteins (TJP) and maintaining intestinal barrier integrity, thereby improving intestinal barrier function.^{27–29} Previous studies have demonstrated that upregulation of the PI3K/AKT/mTOR pathway accelerates LPS-induced intestinal mucosal cell damage, while inhibiting the PI3K/AKT pathway is beneficial for inflammation suppression, enhancing the integrity of intercellular connections in Caco-2 cells and TJPs expression.^{30–32} Inhibiting PI3K/AKT signaling transduction can ameliorate colonic injury.^{33–35} NF- κ B is a crucial transcription factor involved in the inflammatory response, regulating various inflammatory cytokines such as tumor necrosis factor- α (TNF- α), interleukin-6 (IL-6), and interleukin-1 β (IL-1 β).³⁶ Therefore, inhibition of NF- κ B signaling pathway is the key to reducing inflammation. Evidence suggests that the NF- κ B pathway may be activated by the PI3K/AKT pathway, and inhibition of the PI3K/AKT signaling pathway may lead to the blockade of NF- κ B activation.^{31,37} The involvement of the PI3K/AKT/NF- κ B pathway in the pathogenesis of gastrointestinal diseases is evident, and its activation is significantly associated with intestinal barrier damage.³⁸ Experimental studies have shown that inhibition of the PI3K/AKT/NF- κ B pathway can suppress inflammation and intestinal mucosal barrier damage, exerting a protective effect on the intestine.^{38,39} Magnolol and honokiol, the main active components of MO extract, possess various pharmacological activities such as regulating gastrointestinal motility, anti-inflammatory, and anti-oxidative stress effects.⁴⁰ Moreover, MO can repair mucosal damage, protect the intestinal barrier, and regulate intestinal homeostasis.^{40,41} Magnolol reduces intestinal injury by regulating the expression of TNF- α , IL-1 β , and IL-12 through the NF- κ B pathway, while honokiol can reduce colitis in mice by inhibiting the NF- κ B signaling pathway.^{42–44} Additionally, magnolol can inhibit the PI3K/AKT signaling pathway, as evidenced by molecular docking studies showing a strong binding force between magnolol and PI3K.^{45,46} Therefore, inhibiting the PI3K/AKT/NF- κ B pathway may be an effective approach for treating intestinal injury.

Although PT is widely used in medicine, its gastrointestinal side effects have restricted the development and application of new products. Previous studies on the side effects of PT are limited, mainly focusing on gastrointestinal motility disorders, with inadequate research on its damage to intestinal mucosa. Additionally, most studies on the gut microbiota and gastrointestinal diseases have been limited to bacterial aspects. In this study, we explored the efficacy and mechanism of MO in alleviating PT-induced intestinal mucosal damage from multiple perspectives, including inflammation response, oxidative stress, intestinal barrier, gut microbiota (including bacteria and fungi), and signaling pathways validation. This study provides experimental evidence for the rational and safe use of PT.

Materials and Methods

Chemicals and Reagents

Dimethyl sulfoxide (DMSO, batch number: 2021082402), methyl alcohol (batch number: 2022032801), and formic acid (batch number: 2022112001) were purchased from Chengdu Cologne Chemicals Co., Ltd (Sichuan, China). Acetonitrile (Lot No: RBXA1H) was obtained from SK chemicals (Gyeonggi-do, South Korea). Tricaine methanesulfonate (MS-222, RH317149) was sourced from Shanghai Yien Chemical Technology Co., Ltd (Shanghai, China). The Soluble Protein

content (SP) kit (ADS-W-SP002) was provided by Jiangsu Aidisheng Biological Technology Co., Ltd (Jiangsu, China). Zebrafish TNF- α (Lot No: F69008-A), IL-6 (Lot No: F69060-A), IL-1 β (Lot No: F69010-A), superoxide dismutase (SOD, Lot No: F69145-A), catalase (CAT, Lot No: F69795-A), glutathione peroxidase (GSH-Px, Lot No: F69800-A), and malondialdehyde (MDA, Lot No: F69791-A) kits were procured from Shanghai Fanke Industrial Co., Ltd (Shanghai, China). The Animal Total RNA Isolation Kit (Lot. No. R230401), RT Easy™ II (Lot. No. 230501), and Real Time PCR Easy™-SYBR Green I (Lot. No. P230501) were purchased from Chengdu Foregene Co., Ltd (Sichuan, China).

Plant Materials and Ethanolic Extracts Preparation

PT (batch number: 21040101) and MO (batch number: 21060106) were purchased from Sichuan Guoqiang Chinese Herbal Pieces Co., Ltd (Sichuan, China). These batches of PT (report no. 5-273-02-21040101) and MO (report no. 5-259-02-21060106) were found to comply with the standards outlined in the 2020 edition of the Pharmacopoeia of the People's Republic of China (PhC). The herbs were individually powdered and sieved through a No.3 sieve. Subsequently, 200 g of PT and 400 g of MO were each subjected to extraction using a 20-fold volume of 90% ethanol under reflux for three cycles, with each cycle lasting 2 h. The resulting concentrated alcoholic extract underwent filtration and compression using rotary steam under reduced pressure at a temperature of 60°C to obtain a solid substance. The yield was calculated, and the resulting product was stored at -80°C.

Ultra-High Performance Liquid Chromatography-Tandem Triple Quadrupole Mass Spectrometry (UPLC-MS/MS)

Dissolved PT, MO and PT-MO in 70% methanol, respectively, then filtered with 0.22 μ m membranes. A discovery was made within the electrospray ionization (ESI) feature of an ultra-high performance liquid chromatography system (Vanquish, Thermo Scientific, Waltham, MA, USA) coupled with a triple quadrupole mass spectrometry instrument (TSQ Fortis, Thermo Scientific, Waltham, MA, USA). Samples were separated on an Accucore C₁₈ column (3 \times 100 mm, 2.6 μ m) at 40°C, with a flow rate of 0.2 mL/min and a sample volume of 5 μ L. The mobile phase comprised two components: (A) 0.1% formic acid in water and (B) acetonitrile. Gradient elution was achieved using the following procedure: 0-5 min, 2%-10% B; 5-15 min, 10%-30% B; 15-20 min, 30%-50% B; 20-25 min, 50%-70% B; 25-30 min, 70%-95% B; 30-35 min, 95% B. The MS system conditions were as follows: positive ionization at 4000 V, negative ionization at 3500 V, sheath gas at 35 kpa, auxiliary gas at 10 kpa, and gas temperature at 350°C. The data were analyzed using Thermo Scientific Xcalibur (v4.2).

Animals and Experiment

The 3-month-old wild AB zebrafish were purchased from Shanghai Fishbio Co., Ltd (Shanghai, China) and reared in a zebrafish culture system for 7 days. The room temperature was maintained at 28 \pm 0.5°C, while the pH value was controlled within the range of 7.4-7.5, and the conductivity was maintained between 500-550 μ S/cm. Light and dark cycles were alternated for 14 h of light followed by 10 h of darkness, and the zebrafish were fed with artemia at 9:00 AM and 5:00 PM daily. All experimental procedures were approved by the Laboratory Animal Ethics Committee of Chengdu University of TCM (2019-35).

After adaptive feeding, some of the zebrafish were mated, and the fertilized embryos were used to measure gastrointestinal motility. The remaining zebrafish were divided into 11 groups in a randomized manner: the control group, the vehicle control (DMSO) group, the PT (2.5 μ g/mL, 5 μ g/mL, 10 μ g/mL) groups, the MO (5 μ g/mL, 10 μ g/mL, 20 μ g/mL) groups, and the PT-MO (2.5 + 5 μ g/mL, 5 + 10 μ g/mL, 10 + 20 μ g/mL) groups, each containing 60 zebrafish. Zebrafish were continuously exposed to the solution for 3 days, with half of the exposure solution replaced daily. All groups except the group control contained 0.1% DMSO, the control group was exposed to zebrafish aquaculture water, and the DMSO group was exposed to 0.1% DMSO solution. The final volume of solution for all groups remained consistent.

On the 4th day, zebrafish were anesthetized with MS-222 and euthanized in an ice bath. Subsequently, the zebrafish intestine and its contents were collected under sterile conditions. Some tissues were fixed in 4% paraformaldehyde solution for subsequent hematoxylin and eosin (H&E) staining, while others were fixed in 3% glutaraldehyde for

transmission electron microscopy observation. The remaining intestinal tissues and their respective contents were adequately stored at -80°C . Intestinal contents were utilized for the detection of 16S rRNA and metagenomics, whereas intestinal tissues were employed for enzyme-linked immunosorbent assay (ELISA) and quantitative real-time polymerase chain reaction (qRT-PCR).

Gastrointestinal Motility Analysis

Based on the method outlined by Zhou and Wang et al,^{47,48} fertilized embryos should be transferred to 6-well plates on the 5th day of development, with 30 embryos per well. After the fertilized embryos develop to the 5th day, they should be transferred to 6-well plate, 30 tails in each well. Following 16 h of exposure to Nile red solution, the solution is removed, and 3 mL of different drug concentrations are added to each well. Subsequently, photographs are captured using a Leica microscope after 6 h, and the fluorescence intensity of the intestinal tract is analyzed using Image J (NIH, Bethesda, USA). Quantitative assessment is then conducted to evaluate the medication's impact on zebrafish intestinal motility, utilizing the total fluorescence signal derived from the intestine.

Histological Analysis

Following fixation in a 4% paraformaldehyde solution for 48 h, the tissues were dehydrated, embedded, sectioned, and stained using the H&E technique. The photomicrographs were obtained using HS6 microscope (sunny, HK, China).

After immersion in a solution containing 3% glutaraldehyde, the tissues were fixed with 1% osmium tetroxide. Subsequently, they were dehydrated through a series of acetone washes and infiltrated with Epoxy embedding medium (Epoxy) 812 for an extended period. Once fully embedded, semithin sections were stained with methylene blue, while ultrathin sections were carefully sliced using a diamond knife and then stained with uranyl acetate and lead citrate. Finally, the sections were examined using a JEM-1400-FLASH TEM (JEOL, Japan).

16S rRNA Sequencing of the Gut Microbiota

DNA extraction from the intestinal contents was performed using the MagPure Stool DNA KF Kit B (Magen Biotechnology, MD5115-02B). The concentration of DNA was determined using the QubitTM dsDNA BR Assay Kit (Invitrogen, Q32850). The V3-V4 region of bacterial 16S rRNA was targeted for amplification using the 338F forward primer (5'-ACTCTACGGGAGGCAGCAG-3') and the 806R reverse primer (5'-GGACTACHVGGGTWTCTAAT-3'). Purification of PCR amplification products was achieved with Agen court AM Pure XP magnetic beads, followed by dissolution in Elution Buffer. The library construction utilized the Miseq Reagent Kit v3, with subsequent double-ended sequencing on the BGISEQ platform (BGI, Shenzhen, China) generating paired-end reads of 2×300 bp. Raw offline data in fq format were processed using fastqc software (v0.1.2) for each fq file. Data filtering was then conducted, and Fast Length Adjustment of Short reads (FLASH, v1.2.11) was employed to establish the overlapping relationship and assemble the read pairs into Tags. Subsequently, USEARCH (v7.0.1090) was utilized to cluster Tags with 97% similarity into operational taxonomic units (OTUs). Finally, species annotation was performed based on the RDP Release (v11.5, 20160930) database.

Metagenomics Sequencing of the Gut Microbiota

The extraction of total DNA from zebrafish intestinal contents was performed using the Mag Pure Stool DNA KF Kit B (Magen Biotechnology, MD5115-02B). Subsequently, the DNA samples meeting quality standards underwent ultrasonic fragmentation. The fragmented samples then underwent magnetic bead fragment selection, repair of DNA ends, and addition of A bases at the 3' end. The resulting product was then amplified to create a library for sequencing. The initial data was provided in fq format and underwent filtering and quality control using SOAP nuke (v1.5.0) software. Host sequence comparison and removal were conducted using Bowtie2 (v2.2.5), resulting in the generation of Clean Data. The Clean Data, which had undergone quality control and host sequence removal, was subjected to de novo assembly using the MEGAHIT assembly software. Following assembly, the Meta Gene Mark software was employed to predict gene sequences within the contigs. To eliminate redundancy in the gene prediction results, CD-HIT software was utilized. Finally, the Salmon software was employed to calculate the relative abundance of each gene.

Detection of Inflammatory Cytokines and Antioxidant Enzymes by ELISA

Zebrafish intestinal tissues were weighed and homogenized normal saline solution at a 1:10 ratio. After centrifugating, the supernatant was collected to determine the protein concentration. Subsequently, the levels of inflammatory cytokines and antioxidant enzymes in the intestinal tissues were measured according to the manufacturer's instructions provided with the ELISA kits.

qRT-PCR

The Animal Total RNA Isolation Kit was utilized to extract total RNA from intestinal tissues. Subsequently, it was reverse transcribed into cDNA using RT Easy™ II. For qRT-PCR analysis, the provided instructions with Real Time PCR Easy™-SYBR Green I were strictly followed. The reaction procedure included pre-denaturation (95°C, 3 min), denaturation (95°C, 10s), annealing (60°C, 10s), extend (72°C, 20s), and an amplification program consisting of 40 cycles. Additionally, the default melting point curve was utilized. The relative levels of mRNA expression were determined using the $2^{-\Delta\Delta CT}$ method. Specific primer sequences employed in this experiment can be found in Table 1.

Statistical Analysis

The SPSS 26.0 software (IBM Corp., Armonk, NY, USA) was utilized for significant difference analysis. One-way analysis of variance (ANOVA) was employed to analyze differences between multiple groups. $P < 0.05$ or $P < 0.01$ was considered statistically significant. Data visualization was conducted using GraphPad Prism 8.0 (GraphPad, La Jolla, CA, USA).

Result

UPLC-MS/MS Analysis

Qualitative analysis of the extracts revealed representative components in PT and MO, identified by comparing their mass-to-charge ratios with those of reference standards. In PT, the representative components included tenuifolin, polygalaxanthone III, 3,6'-disinapoyl sucrose, and polygalacic acid (Figure 1A and B), while in MO, representative components included magnolol and honokiol (Figure 1C and D). Interestingly, these components were also detected in the PT-MO combination (Figure 1E and F).

MO Ameliorated PT-Induced Intestinal Motility Disorder in Zebrafish

The fluorescence intensity reflects the level of intestinal motility in zebrafish. The minimal difference observed between the control group and the DMSO group suggests that the impact of the solvent on the experiment is negligible. Conversely, the PT group exhibited a dose-dependent increase in fluorescence intensity compared to the DMSO group

Table 1 Oligonucleotide Sequences

Gene Name	Forward Primer	Reverse Primer
<i>illb</i>	TGGACTTCGCAGCACAAAATG	CACTTCACGCTCTTGGATGA
<i>il6</i>	TCAACTTCTCCAGCGTGATG	TCTTTCCCTCTTTTCTCCTG
<i>tnfa</i>	CAATCCGCTCAATCTGCACG	TACAGATGTGTTGGCGGCAC
<i>pik3cb</i>	ACATGGCTCTGCAAGATGCT	GGAGGCATCTCGGACCAAAA
<i>nfkb1</i>	AGGAGCGCAGGATACACAG	CAGGAAACAGCTTCTCCAC
<i>akt1</i>	GCAAGATGTGGATCAGCTGGAG	CCACAGTCTGGATGGCTTGGT
<i>jak3</i>	TGTTTGACAGGGACAGTATG	CCCAGGCACTCATTTTCAAT
<i>ikkb</i>	TGGCTACAGCGACAGCTCTG	GCATTCCAGCGTTCTCTGA
<i>cldn1</i>	CTGCTGTATCTGTGGGAGTGAA	TAATCAGGAGAACAGGCGAAG
<i>odna</i>	TGGACCCTCAAGAGGCGAT	ACATCTTGCGGGGAGTTCTG
<i>tjp1</i>	ACAAGAACAGGGCGGAACAGT	ACCTCCAGAAATCAGCACGA
<i>muc2.1</i>	ACCTTCGATGGGGACGTCTA	GGCAGCGTCACTTTTGCTTC
<i>gapdh</i>	CGTCTTGAGAAACCTGCCAAG	AACCTGGTGCTCCGTGTATC

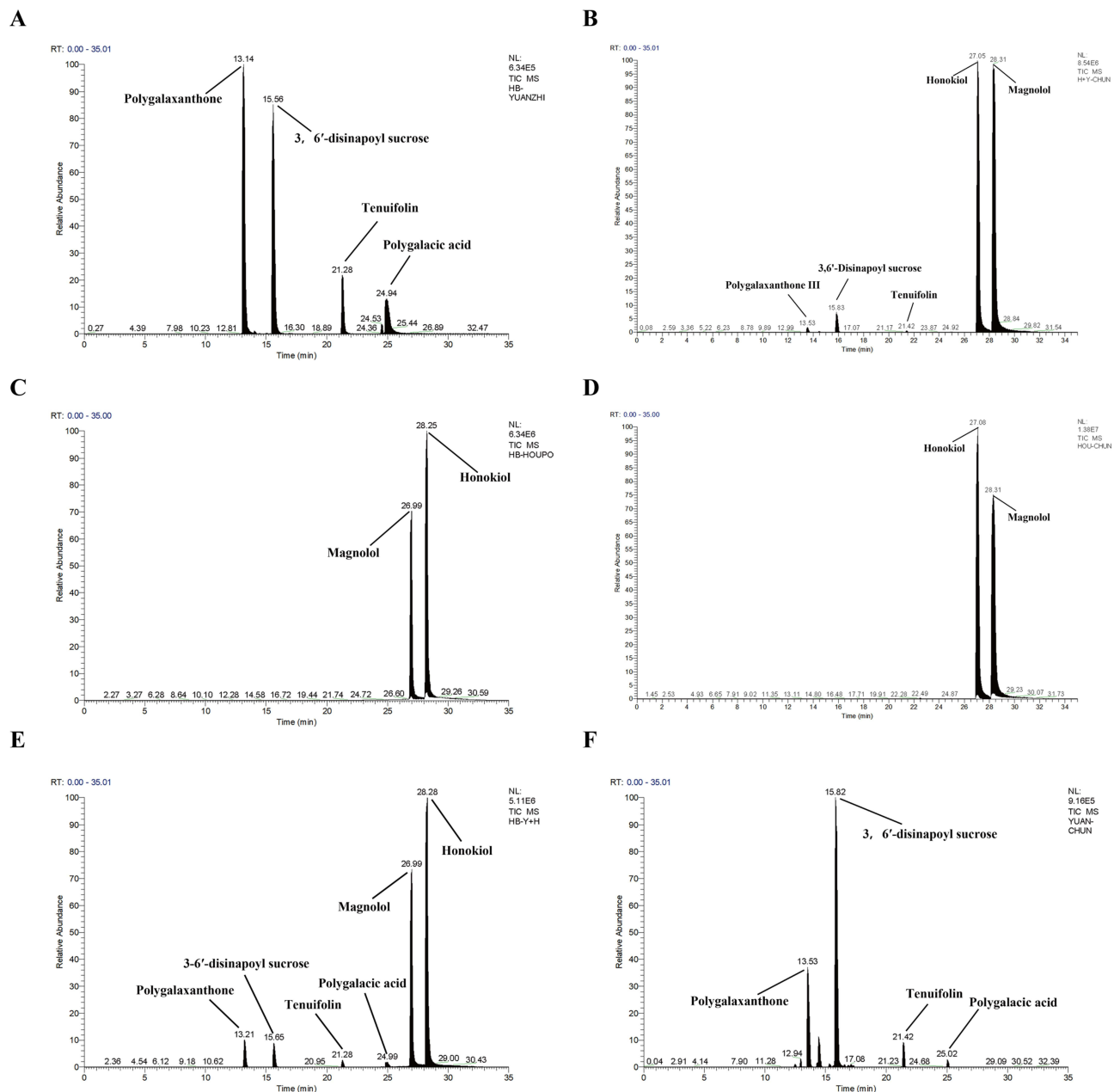


Figure 1 UPLC-MS/MS analysis of PT, MO and PT-MO couple. **(A)** Representative components in standard sample of PT, **(B)** Representative components in PT sample, **(C)** Representative components in standard sample of MO, **(D)** Representative components in MO sample, **(E)** Representative components in standard sample of PT-MO couple, **(F)** Representative components in PT-MO couple sample.

($P < 0.05$, Figure 2). However, the PT-MO group demonstrated significantly lower fluorescence intensity than the PT group ($P < 0.05$). These results indicate that MO has the potential to alleviate PT-induced intestinal peristalsis disorders.

MO Ameliorated the Intestinal Structure Damage in Zebrafish

The results of H&E staining revealed that the intestinal structure of zebrafish in the control and DMSO groups remained intact, with no obvious damage to the intestinal villi observed (Figure 3A). In the low-dose PT group, a few vacuoles were observed along with an increase in goblet cell proliferation. And the medium-dose PT group exhibited detachment of intestinal villi, accompanied by vacuoles and an increase in goblet cell proliferation. In the high-dose PT group, the medium-dose PT group exhibited detachment of intestinal villi, accompanied by vacuoles and an increase in goblet cell

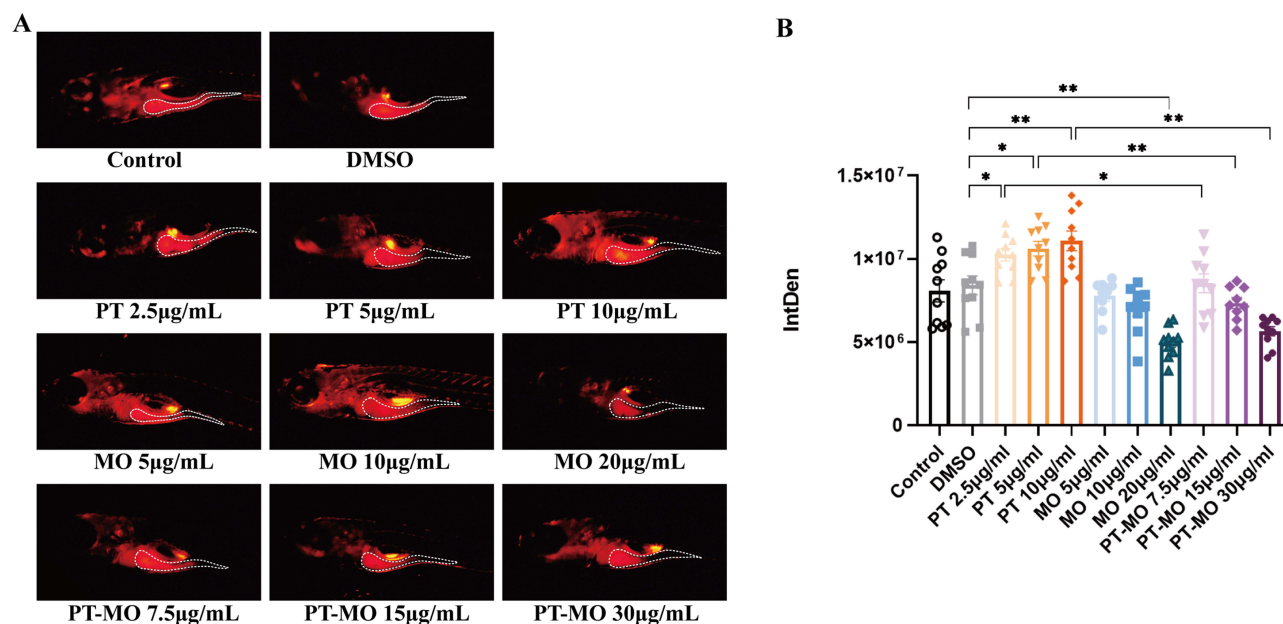


Figure 2 MO ameliorated PT-induced intestinal motility disorder. (A) Representative images of zebrafish intestinal Nile red staining. The white dotted lines indicate the areas used for fluorescence intensity measurement. (B) Quantification of fluorescence intensity. Data are expressed as mean \pm SEM ($n = 10$). * $P < 0.05$, ** $P < 0.01$.

proliferation. The structure of the intestinal villi was disrupted and detached. Notably, PT-MO group did not display significant structural damage.

Simultaneously, the length of intestinal villi was measured (Figure 3B). Compared with the DMSO group, the length of intestinal villi in the PT medium and high dose groups was significantly reduced ($P < 0.05$). Conversely, Compared with PT group, the intestinal villus length in the PT-MO group increased significantly ($P < 0.01$). These results suggest that MO can ameliorate PT-induced intestinal motility disorders and mucosal damage.

MO Alleviated PT-Induced Intestinal Flora Disorder

16S rRNA Analysis

The α -diversity sparse curve based on the number of operational taxonomic units (OTUs) of different samples tends to be stabilize on the right, indicating that the sequencing data has reached saturation (Figure 4A and B). The α diversity analysis based on ACE and Simpson indices showed that MO significantly ameliorated the reduction in species richness caused by PT ($P < 0.01$, Figure 4C and D). Principal Co-ordinates Analysis (PCoA) revealed distinct visual separation between the PT and control groups, with the intestinal flora structure of the PT-MO group deviating from that of the PT group and resembling that of the control group (Figure 4E). The petaline diagram displayed the number of common and unique OTUs in each group, with 409 OTUs shared among the five groups and the PT-MO group exhibiting a richer number of OTUs than the PT group (Figure 4F). These findings suggest that MO has the potential to alleviate the decline in microbial diversity induced by PT.

Further analysis of species composition at different levels revealed alterations in the intestinal microbiota. At the phylum level, *Proteobacteria*, *Fusobacteria*, *Bacteroidetes*, and *Firmicutes* were the dominant flora in the zebrafish intestine (Figure 4G). At the genus level, the relative abundance of *Plesiomonas* in PT group was significantly higher than that in the control group, and MO restored it to normal level ($P < 0.05$). Furthermore, the MO couple markedly enhanced the proportion of beneficial microorganisms such as *Lactobacillus*, *Blautia*, *Barnesiella*, *Chitinibacter* and *Prevotella* ($P < 0.01$, Figure 4H and I). The results demonstrate that MO restored the relative abundance of pathogenic bacteria to normal levels and increased the microbial composition of beneficial bacteria.

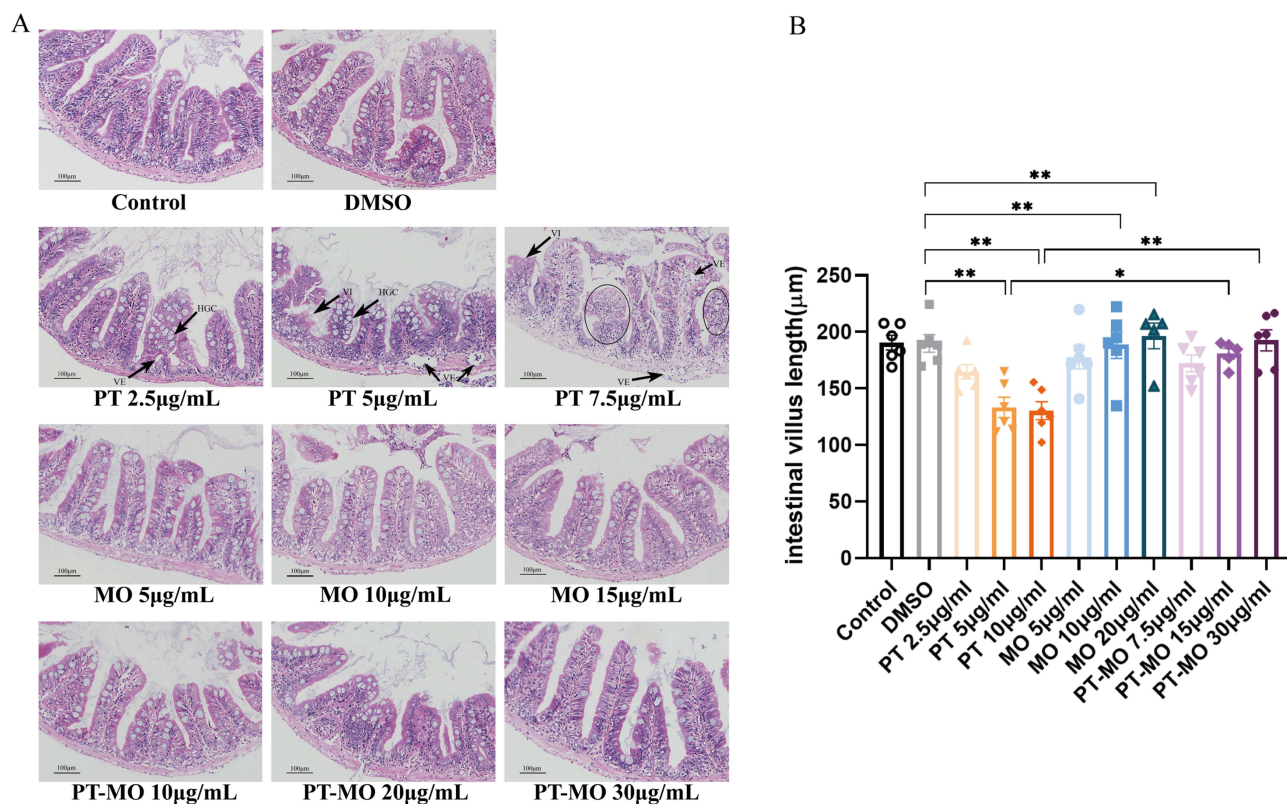


Figure 3 MO ameliorated PT-induced intestinal structural damage. **(A)** Representative images of HE staining (scale bar = 100 µm). **(B)** Quantification of intestinal villus length. HGC indicates goblet cell hyperplasia, VE indicates vacuole, and VI indicates enterochromaffin vacuole. Data are expressed as mean ± SEM (n = 6). * $P < 0.05$, ** $P < 0.01$.

Metagenomics Analysis

Analysis of similarities (Anosim) analysis based on bray-curtis algorithm was conducted to assess whether the variation between groups at each taxonomic level exceeded that within groups. The results indicated that at the phylum ($R = 0.2703$), genus ($R = 0.2844$), and species ($R = 0.2870$) levels, the dissimilarity of bacterial communities between groups was significantly greater than that within groups ($P < 0.05$, Figure 5A). At the phylum level, alongside dominant bacteria like *Proteobacteria*, *Firmicutes*, *Bacteroidetes*, and *Fusobacteria*, the fungal microbiota of zebrafish intestines was predominantly composed of *Ascomycota* and *Basidiomycota* (Figure 5B).

The abundance of microorganisms at the genus and species levels was analyzed using abundance information derived from species annotations. At the genus level, compared to the control group, there was a significant increase in the relative abundance of pathogenic bacteria such as *Aeromonas* and *Shewanella* in the PT group ($P < 0.05$). However, treatment with MO restored their relative abundance. Additionally, MO markedly increased the relative abundance of *Saccharomyces*, *Aspergillus* and *Kluyveromyces* ($P < 0.01$, Figure 5C). At the species level, the relative abundance of *Aeromonas veronii* was significantly higher in the PT group than in the DMSO group ($P < 0.05$), which was mitigated by MO treatment ($P < 0.01$). Furthermore, MO significantly enhanced the relative abundance of *Saccharomyces cerevisiae* and *Kluyveromyces marxianus* ($P < 0.05$, Figure 5D and E).

Linear Discriminant Analysis Effect Size (LEFSE) identified biomarkers with LDA scores > 3 (Figure 5F and G). While *Proteobacteria* exhibited higher relative abundance in the control group, *Aeromonas veronii* emerged as a biomarker in the PT group, whereas *Saccharomycetaceae* and *Kluyveromyces* were biomarkers in the PT-MO group. The impact of MO on the intestinal flora was evident, as it modulated their composition, resulting in an increase in the relative abundance of beneficial bacteria and a decrease in the relative abundance of pathogenic bacteria.

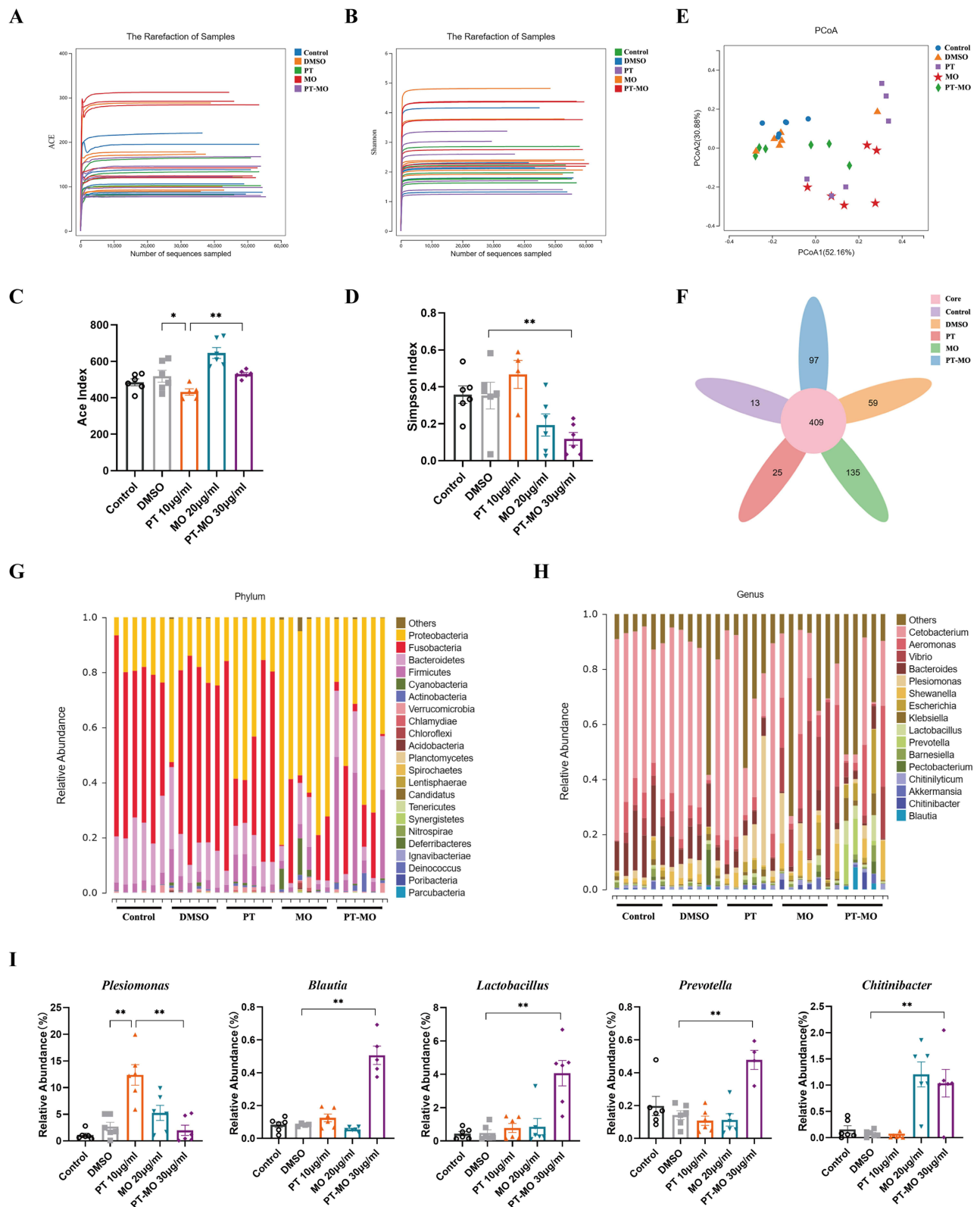


Figure 4 MO alleviated PT-induced intestinal flora disorder. **(A)** ACE diversity sparse curve. **(B)** Shannon diversity sparse curve. **(C)** ACE diversity index based on OUT level. **(D)** Shannon diversity index based on OUT level. **(E)** β -diversity of the gut microbiota based on Principal Co-ordinates Analysis (PCoA) using unweighted unifrac algorithm. **(F)** Petaline diagram of the number of OTUs in each group. **(G)** Columnar diagram of phylum level. **(H)** Columnar diagram of genus level. **(I)** The relative abundance of different kinds of microorganisms were compared among groups. Data are expressed as mean \pm SEM (n = 6). *P < 0.05, **P < 0.01.

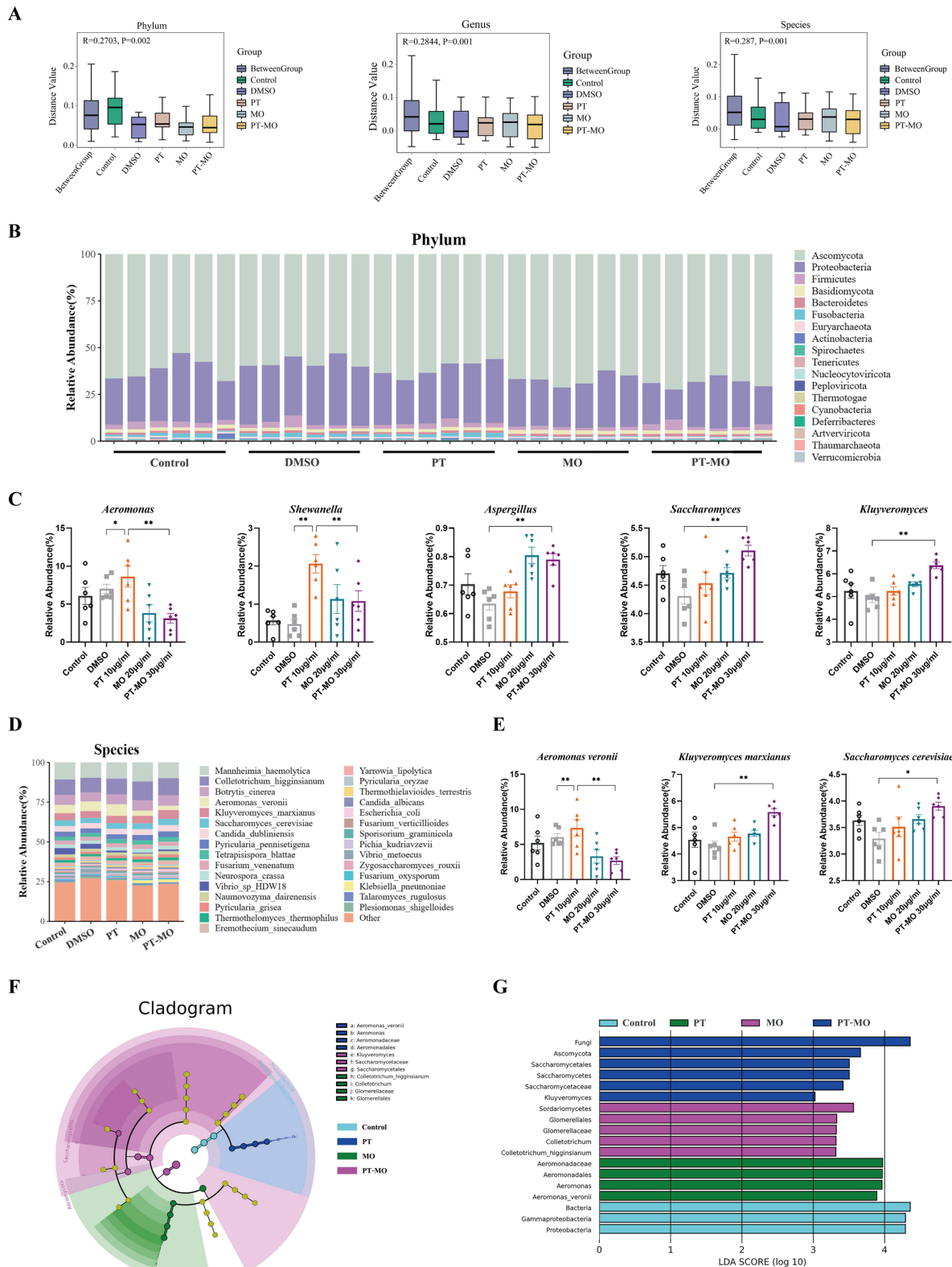


Figure 5 MO alleviated PT-induced intestinal flora disorder. **(A)** β -diversity analysis of microorganisms at phylum, genus and species levels based on bray-curtis distance matrix. **(B)** Columnar diagram of phylum level. **(C)** Differences in relative abundance of microorganisms at the genus level. **(D)** Columnar diagram of species level. **(E)** Differences in relative abundance of microorganisms at the species level. **(F)** LEfSe circular evolutionary branch diagram. **(G)** LEfSe LDA value distribution histogram. Data are expressed as mean \pm SEM (n = 6). * $P < 0.05$, ** $P < 0.01$.

MO Alleviated PT-Induced Inflammation and Oxidative Stress

Research on zebrafish intestine pathology has demonstrated that PT can induce harm to the intestinal mucosa, leading to generalized mucosal damage due to inflammation and oxidative stress. Therefore, we investigated the effects of PT, MO and PT-MO on inflammatory factors and oxidative stress indicators in zebrafish intestinal tissues. In comparison to the DMSO group, the concentrations of IL-1 β , IL-6, TNF- α and MDA were significantly increased in the PT group ($P < 0.05$), whereas MO demonstrated the ability to reduce their expression ($P < 0.01$, **Figure 6A-D**). Additionally, the levels of GSH-Px, CAT and SOD were significantly reduced in the PT group ($P < 0.05$), and MO restored them to levels comparable of DMSO group ($P < 0.01$, **Figure 6E-G**). These findings indicate that MO effectively alleviates PT-induced inflammation and oxidative stress.

MO Ameliorated PT-Induced Intestinal Barrier Damage

Results from TEM revealed abundant microvilli in both the control and DMSO groups, with intact tight intercellular junctions indicating normal functioning and structural integrity. However, in the PT group, mitochondria were swollen, microvilli were sparse or absent, and tight junctions between cells were disrupted. Following MO treatment, intestinal structure damage improved, tight junctions returned to normal, and structural integrity was restored (**Figure 7A**).

To evaluate intestinal barrier function in zebrafish, TJPs (Tight Junction Proteins) and mucin were utilized as important markers. The relative mRNA expression of *cldn1*, *oclna*, *tjp1* and *muc2.1* was significantly decreased in the PT group Compared to the DMSO group ($P < 0.01$, **Figure 7B-E**). Conversely, expression of these genes in the PT-MO group was significantly increased compared to the PT group ($P < 0.01$). These results demonstrate that MO significantly ameliorates intestinal barrier function.

MO Inhibited the Activation of PI3K/AKT/NF- κ B Signaling Pathway

We assessed the gene expression levels of *il1b*, *il6*, and *tnfa*. Compared to the DMSO group, PT induced a significant increase in their expression levels, whereas MO treatment markedly reduced their expression ($P < 0.01$, **Figure 8A-C**). To

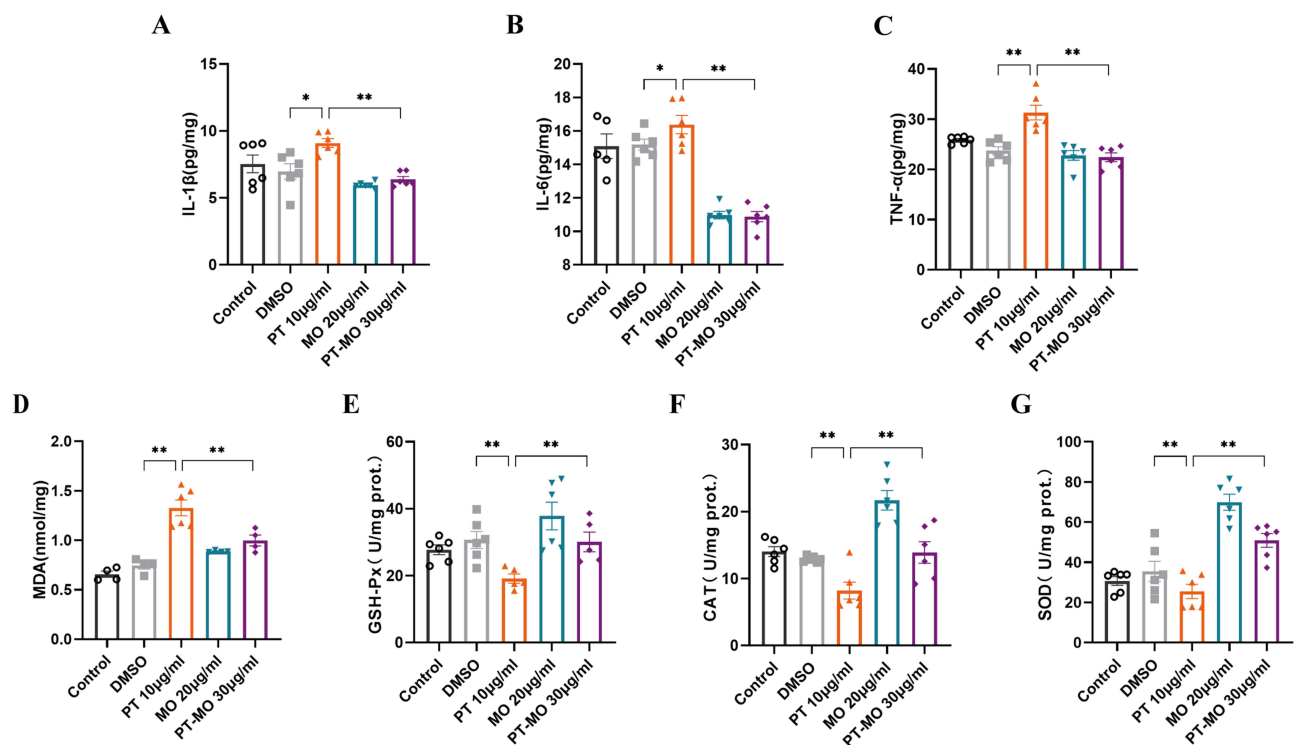


Figure 6 MO alleviated intestinal inflammation and oxidative stress in zebrafish. The expression of inflammatory cytokines (A) IL-1 β , (B) IL-6, (C) TNF- α and markers of oxidative stress (D) MDA, (E) GSH-Px, (F) CAT, (G) SOD in zebrafish intestinal tissue. Data are expressed as mean \pm SEM (n = 6). * $P < 0.05$, ** $P < 0.01$.

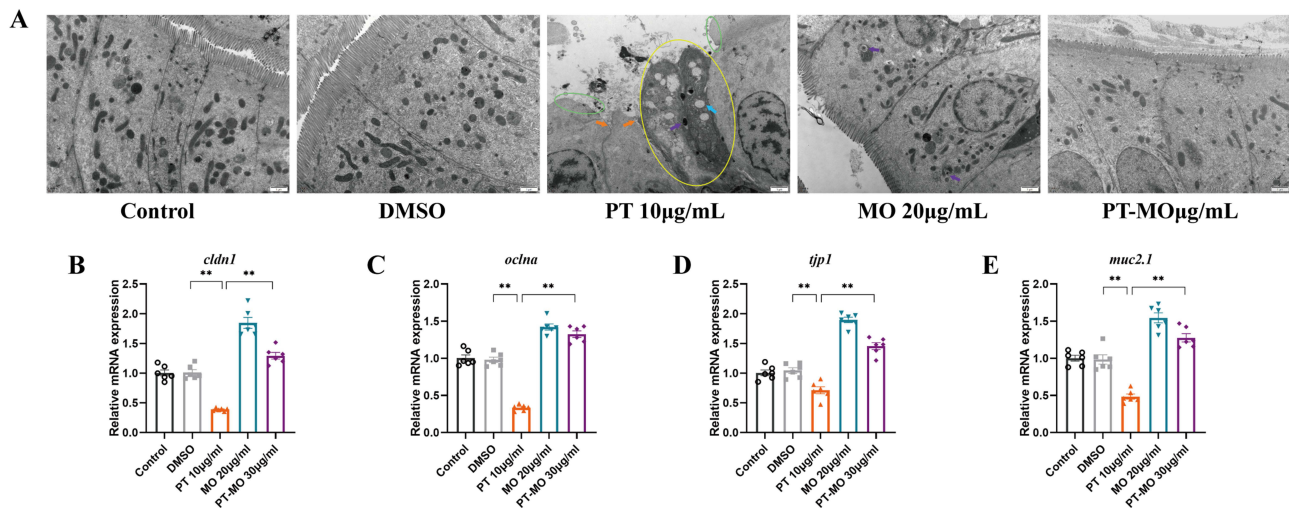


Figure 7 MO protected the intestinal barrier function of zebrafish. **(A)** Representative images of TEM staining (scale bar = 1 µm). The mRNA relative expression of zebrafish intestinal barrier genes **(B)** *cldn1*, **(C)** *oclna*, **(D)** *tjp1* and **(E)** *muc2.1*. Data are expressed as mean ± SEM (n = 6). *P < 0.05, **P < 0.01. Purple circles represent the disappearance of villi, yellow circles represent apoptosis, Orange arrows represent impaired tight junctions, purple arrows represent autophagy, baby blue arrows represent vacuoles.

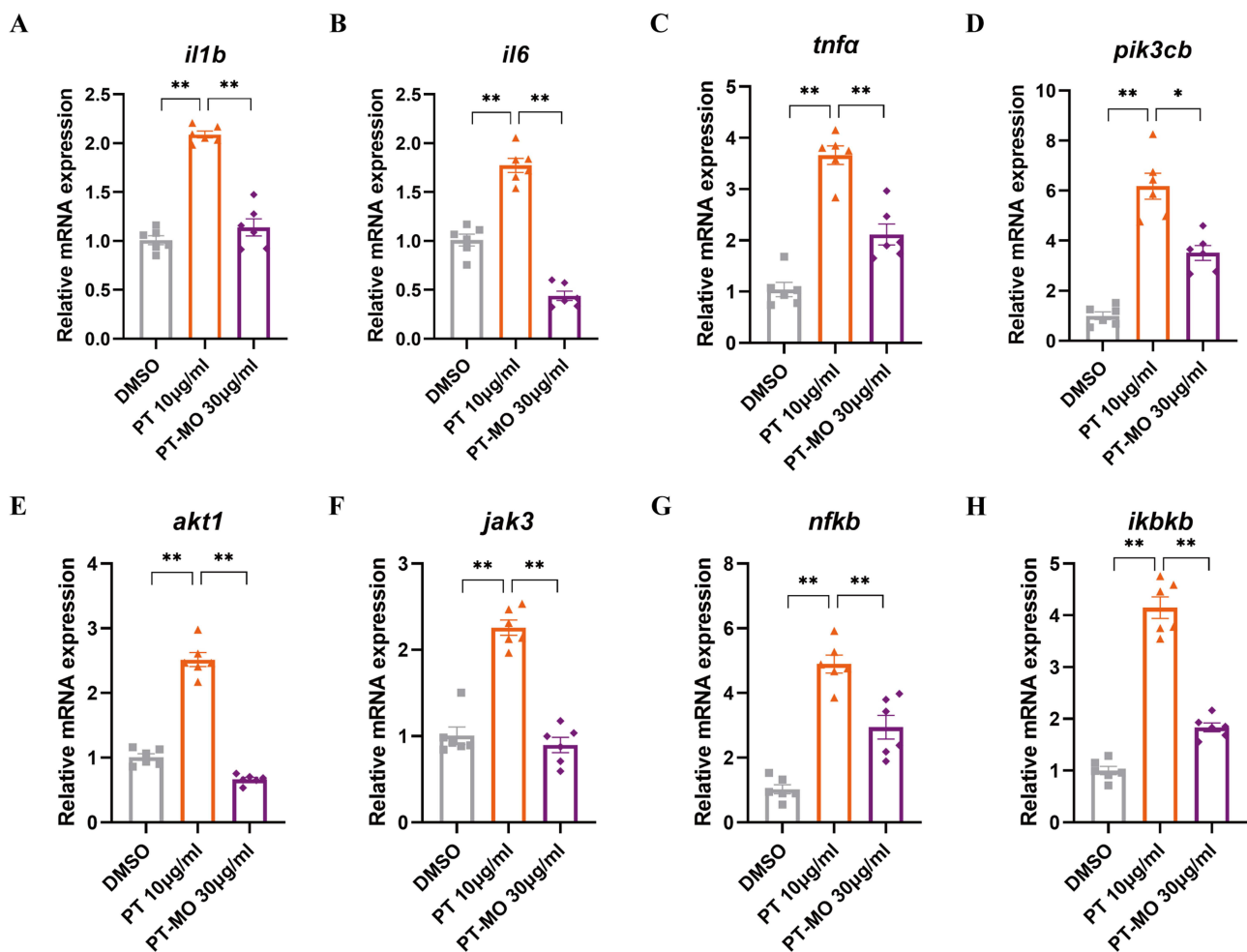


Figure 8 MO inhibited the activation of PI3K/AKT/NF-κB signaling pathway. The mRNA relative expression of **(A)** *il1b*, **(B)** *il6*, **(C)** *tnfa*, **(D)** *pik3cb*, **(E)** *akt1*, **(F)** *jak3*, **(G)** *nfkb*, **(H)** *ikkb*. Data are expressed as mean ± SEM (n = 6). *P < 0.05, **P < 0.01.

delve deeper into the mechanism of MO in mitigating PT-induced intestinal injury, we examined the relative mRNA expression levels of target genes associated with the PI3K/AKT/NF- κ B pathway. In contrast to the DMSO group, the PT group exhibited significantly up-regulated expression levels of *pik3cb*, *akt1*, *jak3*, *nfkb1* and *ikkbk*, all of which were effectively down-regulated by MO treatment ($P < 0.01$, Figure 8D-H), indicating that MO may inhibit the activation of the PI3K/AKT/NF- κ B signaling pathway.

Discussion

PT is utilized to enhance memory and cognitive function. It possesses numerous pharmacological effects, including tranquilizing the mind, improving intelligence, alleviating cognitive impairment, enhancing memory capacity, and exhibiting antidepressant properties.^{49–51} However, the gastrointestinal side effects associated with PT cannot be overlooked. Research indicates that PT exerts evident toxicity on the gastrointestinal tract, leading to significant inhibition of gastrointestinal motility and resulting in noticeable gastrointestinal distension, edema, and thinning of the intestinal wall.⁵² Moreover, PT has been observed to potentially disrupt the composition of gastric parietal cells in mice, inducing infiltration of inflammatory cells into submucosal and muscular layers of the digestive system. This process may also induce vascular congestion and swelling of endothelial cells in the stomach and intestines.⁴ In this study, we investigated the effects of PT on zebrafish, specifically focusing on its impact on mucosal health. We observed that compared to the PT group, the MO group showed significantly decreased levels of IL-1 β , IL-1, and IL-6, while levels of SOD, CAT, GSH-Px, *cldn1*, *oclna*, *muc2.1*, and *tjp1* were increased, demonstrating remarkable anti-inflammatory, antioxidant, and barrier protective effects.

Studies suggest that both bacteria and fungi play roles in regulating host intestinal homeostasis.^{53,54} Intestinal microorganisms create a biological barrier in the intestine to prevent excessive proliferation of foreign pathogenic microorganisms and direct contact between toxins and the mucosa.^{55,56} Dysregulation of the intestinal microbiota can lead to oxidative stress and inflammatory responses, resulting in intestinal dysfunction.⁵⁷ In this study, we detected changes in intestinal microorganisms and observed a decrease in microbial diversity and an increase in the relative abundance of pathogenic bacteria, such as *Plesiomonas*, *Aeromonas*, *Aeromonas veronii*, and *Shewanella*, following PT treatment. *Plesiomonas* is an opportunistic pathogen causing intestinal infections in zebrafish, and *Plesiomonas shigelloides* is also implicated in “winter diseases”.^{58,59} Aerolysin secreted by *Aeromonas veronii* can cause serious damage to the zebrafish intestine. LEFSE analysis identified *Aeromonas veronii* as a biomarker for the PT group. After MO treatment, the biomarkers shifted to *Saccharomyces* and *Kluyveromyces*, accompanied by a reduction in the relative abundance of pathogenic bacteria, suggesting their role in intestinal damage prevention. Furthermore, MO increased the relative abundance of beneficial bacteria such as *Prevotella*, *Lactobacillus*, *Blautia*, *Barnesiella*, *Chitinibacter*, *Kluyveromyces*, *Aspergillus*, *Saccharomyces*, *Saccharomyces cerevisiae*, *Kluyveromyces marxianus*. The cell wall of *Saccharomyces cerevisiae* is crucial for regulating animal intestinal microbial structure, maintaining intestinal epithelial morphology, and regulating immune function, which can enhance the production of anti-inflammatory cytokine IL-10 and decrease levels of inflammatory cytokines IL-6 and TNF- α , thereby improving overall host immunity.^{60–62} *Aspergillus* metabolites can ameliorate intestinal inflammation and mucosal repair. *Pichia* can antagonize other pathogenic fungi such as *Candida*, *Cryptococcus* and *Fusarium*.⁶³ These findings collectively demonstrate that MO protects the intestine from damage by modulating the gut microbiota.

The PI3K/AKT pathway is a classic intracellular signaling pathway that responds to extracellular signals and promotes metabolism, proliferation, and cell survival.⁶⁴ In the pathogenesis of gastrointestinal diseases, activation of the PI3K/AKT pathway induces immune system imbalance and affects the expression of cytokines and oxidative stress. Evidence suggests that inhibiting the PI3K/AKT pathway can significantly alleviate intestinal damage in mice with oxidative stress-induced colitis.⁶⁵ Similarly, it can also regulate inflammation response and oxidative stress in mice with ulcerative colitis.⁶⁶ NF- κ B is a typical inflammatory pathway that can induce inflammatory responses by activating pro-inflammatory cytokines TNF- α , IL-1 β , and IL-6 in cells.⁶⁷ MO can inhibit the activation of NF- κ B pathway and reduce the production of pro-inflammatory cytokines. Therefore, we detected the related target genes of the NF- κ B pathway and its upstream pathway PI3K/AKT, and found that MO can inhibit their expression and thus exert anti-inflammatory effects, which is consistent with the findings of previous research.^{68–70} Additionally, the inflammatory response can induce pathological changes in the intestinal tight junction barrier, leading to intestinal barrier dysfunction, and intestinal barrier damage will promote the up-regulation of pro-inflammatory cytokines,

forming a vicious cycle.^{71,72} In this study, MO downregulated the expression of inflammatory factors, which is conducive to the restoration of intestinal barrier function. The increase in mRNA expression of tight junctions also confirms this. Therefore, inhibiting the PI3K/AKT/NF- κ B pathway may be key to alleviating inflammation, reducing intestinal permeability, and exerting therapeutic effects on the intestine.

Conclusion

In this study, we have demonstrated that high doses of PT indeed have certain adverse effects on the intestines. MO effectively ameliorated PT-induced intestinal damage, resulting in histopathological alterations and reduced expression of pro-inflammatory cytokines and oxidative stress markers. Our experiments indicate that MO improves PT-induced intestinal injury by inhibiting the PI3K/AKT/NF- κ B pathway and restoring intestinal barrier integrity, thereby protecting intestinal epithelial cells from PT-induced intestinal damage.

Abbreviations

ANOVA, analysis of variance; CAT catalase; DMSO, dimethyl sulfoxide; ELISA, enzyme-linked immunosorbent assay; Epoxy, Epoxy embedding medium; ESI, electrospray ionization; GSH-Px, glutathione peroxidase; H&E, hematoxylin and eosin; IL-1 β , interleukin-1 β ; IL-6, interleukin-6; LEFSE, linear discriminant analysis effect size; MDA, malondialdehyde; NF- κ B, nuclear factor kappa B; OTU operational taxonomic unit; PCoA, principal co-ordinates analysis; PhC, pharmacopoeia of the people's republic of China; PI3K/AKT, phosphoinositide 3-kinase/protein kinase B; qRT-PCR, quantitative real time polymerase chain reaction; SOD, superoxide dismutase; TCM, traditional Chinese medicine; TJP, tight junction protein; TNF- α , tumor necrosis factor- α ; UPLC-MS/MS, ultra-high performance liquid chromatography-tandem triple quadrupole mass Spectrometry.

Data Sharing Statement

The datasets PRJNA1054352 and PRJNA1054761 for this study can be found in the National Center for Biotechnology Information (NCBI). <https://www.ncbi.nlm.nih.gov/sra/PRJNA1054352> and <https://www.ncbi.nlm.nih.gov/sra/PRJNA1054761>.

Funding

This research was funded by the National Natural Science Foundation of China (Grant Nos. 82003965 and 82022072), improvement plan of “Xinglin scholar” scientific research talent, Chengdu University of Traditional Chinese Medicine (Grant Nos. XKTD2023002 and QJRC2022033) and the State Administration of Traditional Chinese Medicine of the People's Republic of China.

Disclosure

The authors report no conflicts of interest in this work.

References

1. Wang L, Jin G, Yu H, et al. Protective effects of tenuifolin isolated from *Polygala tenuifolia* Willd roots on neuronal apoptosis and learning and memory deficits in mice with Alzheimer's disease. *Food Funct*. 2019;10(11):7453–7460.
2. Zhang L, Yong Y, Deng L, et al. Therapeutic potential of *Polygala* saponins in neurological diseases. *Phytomedicine*. 2023;108:154483.
3. Cui Y, Zhao X, Tang Y, Zhang Y, Sun L, Zhang X. Comparative Study on the Chemical Components and Gastrointestinal Function on Rats of the Raw Product and Licorice-Simmered Product of *Polygala tenuifolia*. *Evid Based Complement Alternat Med*. 2021;2021:8855536.
4. Wang R, Wu T, Liu Y, Yu MX, Tao XJ, Wang HB. The effect of Radix *Polygala* and honey stir-baking Radix *Polygala* on acute gastrointestinal toxicity of mice. *Chine Med Modern Distance Educ China*. 2018;16(08):88–90.
5. Wang J, Guo J, Liu XW, Yang CM. Effects of raw *Polygala tenuifolia* and different compatibility ratios with *Glycyrrhizae Radix* on gastrointestinal motility in mice. *Pharmacol Clin Chin Mater Med*. 2002;1(5):27–28.
6. Tian H, Wu Y, Wang J, Xia HL. Study on acute toxicity of total saponins, alkaloids, ketones and fatty oils in shengyuanzhi. *Pharmacol Clin Chin Mater Med*. 2005;1(4):50–51.
7. Guan SJ, Yan XP, Lin JK, Li L. Study on acute toxicity test of different processed products of Radix *polygalae*. *Chin J Integr Tradit West Med Intensive Crit Care*. 2012;32(03):398–401.

8. Wen L, Xia N, Tang P, et al. The gastrointestinal irritation of polygala saponins and its potential mechanism in vitro and in vivo. *Biomed Res Int.* 2015;2015:918048.
9. Min-Soo K, Jungim K, Kang-In L, et al. Magnolia officinalis bark extract improves depressive-like behavior in DSS-induced colitis mice. *J Funct Foods.* 2023;108.
10. Ma R, Xie Q, Wang J, Huang L, Guo X, Fan Y. Combination of urine and faeces metabolomics to reveal the intervention mechanism of Polygala tenuifolia compatibility with Magnolia officinalis on gastrointestinal motility disorders. *J Pharm Pharmacol.* 2020;73(2):247–262.
11. Zhang ZH, Wen L, Chen HY, et al. Common combinations of Polygalae Radix. *Chin J Exp Tradit Med Formulae.* 2016;22(12):224–228.
12. Tremaroli V, Bäckhed F. Functional interactions between the gut microbiota and host metabolism. *Nature.* 2012;489(7415):242–249.
13. Nobuhiko K, Sang-Uk S, Cg Y, Gabriel N. Role of the gut microbiota in immunity and inflammatory disease. *Nat Rev Immunol.* 2013;13(5):321–335.
14. Li Z, Wen Q, Pi J, et al. An inulin-type fructan isolated from Serratula chinensis alleviated the dextran sulfate sodium-induced colitis in mice through regulation of intestinal barrier and gut microbiota. *Carbohydr Polym.* 2023;320:121206.
15. Wen X, Wan F, Wu Y, et al. Caffeic acid supplementation ameliorates intestinal injury by modulating intestinal microbiota in LPS-challenged piglets. *Food Funct.* 2023;14(16):7705–7717.
16. Fan Q, Du E, Chen F, et al. Maternal Magnolol Supplementation during Pregnancy and Lactation Promotes Antioxidant Capacity, Improves Gut Health, and Alters Gut Microbiota and Metabolites of Weanling Piglets. *Metabolites.* 2023;13(7):797.
17. Chen F, Zhang H, Du E, et al. Supplemental magnolol or honokiol attenuates adverse effects in broilers infected with Salmonella pullorum by modulating mucosal gene expression and the gut microbiota. *J Anim Sci Biotechnol.* 2021;12(1):87.
18. Huang B, Gui M, An H, et al. Babao Dan alleviates gut immune and microbiota disorders while impacting the TLR4/MyD88/NF-κB pathway to attenuate 5-Fluorouracil-induced intestinal injury. *Biomed Pharmacother.* 2023;166:115387.
19. Feng W, Liu J, Huang L, Tan Y, Peng C. Gut microbiota as a target to limit toxic effects of traditional Chinese medicine: implications for therapy. *Biomed Pharmacother.* 2021;133:111047.
20. Lemme-Dumit JM, Song Y, Lwin HW, et al. Altered Gut Microbiome and Fecal Immune Phenotype in Early Preterm Infants With Leaky Gut. *Front Immunol.* 2022;13:815046.
21. Gong S, Zheng J, Zhang J, Han J. Arabinogalactan ameliorates benzo[a]pyrene-induced intestinal epithelial barrier dysfunction via AhR/MAPK signaling pathway. *Int J Biol Macromol.* 2023;242(Pt 4):124866.
22. Chen S, Li X, Wang Y, et al. Ginsenoside Rb1 attenuates intestinal ischemia/reperfusion-induced inflammation and oxidative stress via activation of the PI3K/Akt/Nrf2 signaling pathway. *Mol Med Rep.* 2019;19(5):3633–3641.
23. Almoiliqy M, Wen J, Xu B, et al. Cinnamaldehyde protects against rat intestinal ischemia/reperfusion injuries by synergistic inhibition of NF-κB and p53. *Acta Pharmacol Sin.* 2020;41(9):1208–1222.
24. Zaghoul MS, Elshal M, Abdelmageed ME. Preventive empagliflozin activity on acute acetic acid-induced ulcerative colitis in rats via modulation of SIRT-1/PI3K/AKT pathway and improving colon barrier. *Environ Toxicol Pharmacol.* 2022;91:103833.
25. Cheng W, Wang X, Wu Y, et al. Huanglian-Houpo extract attenuates DSS-induced UC mice by protecting intestinal mucosal barrier and regulating macrophage polarization. *J Ethnopharmacol.* 2023;307:116181.
26. Shao R, Yang Z, Zhang W, et al. Pachymic acid protects against Crohn's disease-like intestinal barrier injury and colitis in mice by suppressing intestinal epithelial cell apoptosis via inhibiting PI3K/AKT signaling. *Nan Fang Yi Ke Da Xue Xue Bao.* 2023;43(6):935–942.
27. Little D, Dean RA, Young KM, et al. PI3K signaling is required for prostaglandin-induced mucosal recovery in ischemia-injured porcine ileum. *Am J Physiol Gastrointest Liver Physiol.* 2003;284(1):G46–56.
28. Yan H, Ajuwon KM. Butyrate modifies intestinal barrier function in IPEC-J2 cells through a selective upregulation of tight junction proteins and activation of the Akt signaling pathway. *PLoS One.* 2017;12(6):e0179586.
29. Chen S, Huang J, Liu T, et al. PI3K/Akt signaling pathway mediates the effect of low-dose boron on barrier function, proliferation and apoptosis in rat intestinal epithelial cells. *Sci Rep.* 2024;14(1):393.
30. Li N, Neu J. Glutamine deprivation alters intestinal tight junctions via a PI3-K/Akt mediated pathway in Caco-2 cells. *J Nutr.* 2009;139(4):710–714.
31. Zhang B, Wei X, Ding M, Luo Z, Tan X, Zheng Z. Daidzein Protects Caco-2 Cells against Lipopolysaccharide-Induced Intestinal Epithelial Barrier Injury by Suppressing PI3K/AKT and P38 Pathways. *Molecules.* 2022;27(24):8928.
32. Guo H, Gao J, Qian Y, et al. miR-125b-5p inhibits cell proliferation by targeting ASCT2 and regulating the PI3K/AKT/mTOR pathway in an LPS-induced intestinal mucosa cell injury model. *Exp Ther Med.* 2021;22(2):838.
33. Li C, Wang L, Zhao J, et al. Lonicera rupicola Hook.f. et Thoms flavonoids ameliorated dysregulated inflammatory responses, intestinal barrier, and gut microbiome in ulcerative colitis via PI3K/AKT pathway. *Phytomedicine.* 2022;104:154284.
34. Gao HN, Hu H, Wen PC, et al. Yak milk-derived exosomes alleviate lipopolysaccharide-induced intestinal inflammation by inhibiting PI3K/AKT/C3 pathway activation. *J Dairy Sci.* 2021;104(8):8411–8424.
35. Li C, Gong L, Jiang Y, et al. Sanguisorba officinalis ethyl acetate extract attenuates ulcerative colitis through inhibiting PI3K-AKT/NF-κB/STAT3 pathway uncovered by single-cell RNA sequencing. *Phytomedicine.* 2023;120:155052.
36. Wang Y, Du P, Jiang D. Berberine functions as a negative regulator in lipopolysaccharide-induced sepsis by suppressing NF-κB and IL-6 mediated STAT3 activation. *Pathog Dis.* 2020;78(7):ftaa047.
37. Li Y, Ding Q, Gao J, et al. Novel mechanisms underlying inhibition of inflammation-induced angiogenesis by dexamethasone and gentamicin via PI3K/AKT/NF-κB/VEGF pathways in acute radiation proctitis. *Sci Rep.* 2022;12(1):14116.
38. Chen J, Li M, Chen R, et al. Gegen Qinlian standard decoction alleviated irinotecan-induced diarrhea via PI3K/AKT/NF-κB axis by network pharmacology prediction and experimental validation combination. *Chin Med.* 2023;18(1):46.
39. Cheng X, Cao Z, Luo J, et al. Baicalin ameliorates APEC-induced intestinal injury in chicks by inhibiting the PI3K/AKT-mediated NF-κB signaling pathway. *Poult Sci.* 2022;101(1):101572.
40. Niu L, Hou Y, Jiang M, Bai G. The rich pharmacological activities of Magnolia officinalis and secondary effects based on significant intestinal contributions. *J Ethnopharmacol.* 2021;281:114524.
41. Qian X, Hongyan L, Rong M, et al. Effect of Coptis chinensis franch and Magnolia officinalis on intestinal flora and intestinal barrier in a TNBS-induced ulcerative colitis rats model. *Phytomedicine.* 2022;97:153927.

42. Shen P, Zhang Z, He Y, et al. Magnolol treatment attenuates dextran sulphate sodium-induced murine experimental colitis by regulating inflammation and mucosal damage. *Life Sci.* 2018;196:69–76.
43. Xia T, Zhang J, Han L, et al. Protective effect of magnolol on oxaliplatin-induced intestinal injury in mice. *Phytother Res.* 2019;33(4):1161–1172.
44. Wang N, Kong R, Han W, et al. Honokiol alleviates ulcerative colitis by targeting PPAR- γ -TLR4-NF- κ B signaling and suppressing gasdermin-D-mediated pyroptosis in vivo and in vitro. *Int Immunopharmacol.* 2022;111:109058.
45. Yang J, Zou Y, Jiang D. Honokiol suppresses proliferation and induces apoptosis via regulation of the miR-21/PTEN/PI3K/AKT signaling pathway in human osteosarcoma cells. *Int J Mol Med.* 2018;41(4):1845–1854.
46. Hu Z-C, Luo Z-C, Jiang B-J, et al. The Protective Effect of Magnolol in Osteoarthritis: in vitro and in vivo Studies. *Front Pharmacol.* 2019;10:393.
47. Wang T, Dai MZ, Liu FS, et al. Probiotics Modulate Intestinal Motility and Inflammation in Zebrafish Models. *Zebrafish.* 2020;17(6):382–393.
48. Zhou J, Guo SY, Zhang Y, Li CQ. Human prokinetic drugs promote gastrointestinal motility in zebrafish. *Neurogastroenterol Motil.* 2014;26(4):589–595.
49. Jiang N, Zhang Y, Yao C, et al. Tenuifolin ameliorates the sleep deprivation-induced cognitive deficits. *Phytother Res.* 2023;37(2):464–476.
50. Ren H, Gao S, Wang S, et al. Effects of Dangshen Yuanzhi Powder on learning ability and gut microflora in rats with memory disorder. *J Ethnopharmacol.* 2022;296:115410.
51. Zhou Y, Yan M, Pan R, et al. Radix Polygalae extract exerts antidepressant effects in behavioral despair mice and chronic restraint stress-induced rats probably by promoting autophagy and inhibiting neuroinflammation. *J Ethnopharmacol.* 2021;265:113317.
52. Xin Z, Yueli C, Peng W, et al. Polygalae Radix: a review of its traditional uses, phytochemistry, pharmacology, toxicology, and pharmacokinetics. *Fitoterapia.* 2020;147:104759.
53. Doron I, Leonardi I, Li XV, et al. Human gut mycobiota tune immunity via CARD9-dependent induction of anti-fungal IgG antibodies. *Cell.* 2021;184(4):1017–1031.e14.
54. Sender R, Fuchs S, Milo R. Are We Really Vastly Outnumbered? Revisiting the Ratio of Bacterial to Host Cells in Humans. *Cell.* 2016;164(3):337–340.
55. Matson V, Chervin C, Gajewski T. Cancer and the Microbiome-Influence of the Commensal Microbiota on Cancer, Immune Responses, and Immunotherapy. *Gastroenterology.* 2021;160(2):600–613.
56. Anhê FF, Barra NG, Cavallari JF, Henriksbo BD, Schertzer JD. Metabolic endotoxemia is dictated by the type of lipopolysaccharide. *Cell Rep.* 2021;36(11):109691.
57. Drolia R, Bhunia AK. Crossing the Intestinal Barrier via Listeria Adhesion Protein and Internalin A. *Trends Microbiol.* 2019;27(5):408–425.
58. Miller RA, Harbottle H, Aarestrup FM, Schwarz S, Shen J, Cavaco L. Antimicrobial Drug Resistance in Fish Pathogens. *Microbiol Spectr.* 2018;6(1).
59. Egerton S, Culloty S, Whooley J, Stanton C, Ross RP. The Gut Microbiota of Marine Fish. *Front Microbiol.* 2018;9:873.
60. Ardiani A, Higgins JP, Hodge JW. Vaccines based on whole recombinant *Saccharomyces cerevisiae* cells. *FEMS Yeast Res.* 2010;10(8):1060–1069.
61. Harry S, Valentin L, Hugues A, et al. Fungal microbiota dysbiosis in IBD. *Gut.* 2017;66(6):1039–1048.
62. Menezes AGT, Melo DS, Ramos CL, Moreira SI, Alves E, Schwan RF. Yeasts isolated from Brazilian fermented foods in the protection against infection by pathogenic food bacteria. *Microb Pathog.* 2020;140:103969.
63. Mukherjee PK, Chandra J, Retuerto M, et al. Oral mycobiome analysis of HIV-infected patients: identification of *Pichia* as an antagonist of opportunistic fungi. *PLoS Pathog.* 2014;10(3):e1003996.
64. Jiang N, Dai Q, Su X, Fu J, Feng X, Peng J. Role of PI3K/AKT pathway in cancer: the framework of malignant behavior. *Mol Biol Rep.* 2020;47(6):4587–4629.
65. Yan S, Hui Y, Li J, Xu X, Li Q, Wei H. Glutamine relieves oxidative stress through PI3K/Akt signaling pathway in DSS-induced ulcerative colitis mice. *Iran J Basic Med Sci.* 2020;23(9):1124–1129.
66. Li F, Yang Y, Ge J, et al. Multi-omics revealed the mechanisms of *Codonopsis pilosula* aqueous extract in improving UC through blocking abnormal activation of PI3K/Akt signaling pathway. *J Ethnopharmacol.* 2024;319(Pt 2):117220.
67. Yu C, Wang D, Tong Y, et al. Trans-Anethole Alleviates Subclinical Necro-Haemorrhagic Enteritis-Induced Intestinal Barrier Dysfunction and Intestinal Inflammation in Broilers. *Front Microbiol.* 2022;13:831882.
68. Liu B, Piao X, Niu W, et al. Kuijieyuan Decoction Improved Intestinal Barrier Injury of Ulcerative Colitis by Affecting TLR4-Dependent PI3K/AKT/NF- κ B Oxidative and Inflammatory Signaling and Gut Microbiota. *Front Pharmacol.* 2020;11:1036.
69. Piao X, Liu B, Sui X, et al. Picoside II Improves Severe Acute Pancreatitis-Induced Intestinal Barrier Injury by Inactivating Oxidative and Inflammatory TLR4-Dependent PI3K/AKT/NF- κ B Signaling and Improving Gut Microbiota. *Oxid Med Cell Longev.* 2020;2020:3589497.
70. Xu H, Wang Y, Jurutka PW, et al. 16 α -Hydroxytrametenolic Acid from *Poria cocos* Improves Intestinal Barrier Function Through the Glucocorticoid Receptor-Mediated PI3K/Akt/NF- κ B Pathway. *J Agric Food Chem.* 2019;67(39):10871–10879.
71. Gong S, Zheng J, Zhang J, et al. Taxifolin ameliorates lipopolysaccharide-induced intestinal epithelial barrier dysfunction via attenuating NF- κ B/MLCK pathway in a Caco-2 cell monolayer model. *Food Res Int.* 2022;158:111502.
72. Wu Y, Cheng B, Ji L, et al. Dietary lysozyme improves growth performance and intestinal barrier function of weaned piglets. *Anim Nutr.* 2023;14:249–258.

Drug Design, Development and Therapy

Dovepress

Publish your work in this journal

Drug Design, Development and Therapy is an international, peer-reviewed open-access journal that spans the spectrum of drug design and development through to clinical applications. Clinical outcomes, patient safety, and programs for the development and effective, safe, and sustained use of medicines are a feature of the journal, which has also been accepted for indexing on PubMed Central. The manuscript management system is completely online and includes a very quick and fair peer-review system, which is all easy to use. Visit <http://www.dovepress.com/testimonials.php> to read real quotes from published authors.

Submit your manuscript here: <https://www.dovepress.com/drug-design-development-and-therapy-journal>